Author Manuscript

Author Manuscript

Author Manuscript

Author Manuscript

HHS Public Access

Author manuscript

Biochim Biophys Acta Gen Subj. Author manuscript; available in PMC 2024 August 01.

Published in final edited form as:

Biochim Biophys Acta Gen Subj. 2023 August ; 1867(8): 130374. doi:10.1016/j.bbagen.2023.130374.

Anaphylatoxin C5a receptor signaling induces mitochondrial fusion and sensitizes Retina Pigment Epithelial Cells to oxidative stress

Masaaki Ishii[1,*], **Bärbel Rohrer**[1,2,*]

[1]Department of Ophthalmology, Medical University of South Carolina, Charleston, SC, 29425, USA

[2]Ralph H. Johnson VA Medical Center, Charleston, SC, 29401, USA; Department of Neurosciences, Medical University of South Carolina, Charleston, SC, 29425, USA

Abstract

Mitochondrial dynamics is a morphological balance between fragmented and elongated shapes, reflecting mitochondrial metabolic status, cellular damage, and mitochondrial dysfunction. The anaphylatoxin C5a derived from complement component 5 cleavage, enhances cellular responses involved in pathological stimulation, innate immune responses, and host defense. However, the specific response of C5a and its receptor, C5a receptor (C5aR), in mitochondria is unclear. Here, we tested whether the C5a/C5aR signaling axis affects mitochondrial morphology in human-derived retinal pigment epithelial cell monolayers (ARPE-19). C5aR activation with the C5a polypeptide-induced mitochondrial elongation. In contrast, oxidatively stressed cells (H_2O_2) responded to C5a with an enhancement of mitochondrial fragmentation and an increase in the number of pyknotic nuclei. C5a/C5aR signaling increased the expression of mitochondrial fusion-related protein, mitofusin-1 (MFN1) and −2 (MFN2), as well as enhanced optic atrophy-1 (Opa1) cleavage, which are required for mitochondrial fusion events, whereas the mitochondrial fission protein, dynamin-related protein-1 (Drp1), and mitogen-activated protein kinase (MAPK)-dependent extracellular signal−regulated protein kinase (Erk1/2) phosphorylation were not affected. Moreover, C5aR activation increased the frequency of endoplasmic reticulum (ER)-mitochondria contacts. Finally, oxidative stress induced in a single cell within an RPE monolayer (488 nm blue laser spot stimulation) induced a bystander effect of mitochondrial fragmentation

*Addresses for correspondence: BR: Department of Ophthalmology, Medical University of South Carolina, 167 Ashley Avenue, Charleston, SC 29425; phone: (843) 792-5086; fax (843) 792-1723; rohrer@musc.edu, MI: Department of Ophthalmology, Medical University of South Carolina, 167 Ashley Avenue, Charleston, SC 29425; phone: (843) 792-2166; fax (843) 792-1166; ishiim@musc.edu.

Declaration of interests

The authors declare that they have no known competing financial interests or personal relationships that could have appeared to influence the work reported in this paper.

Credit author statement

Author 1 Masaaki Ishii: Conceptualization, Methodology, formal analysis, data curation, writing original draft, visualization. Author 2 Bärbel Rohrer: Conceptualization, writing review and editing, resources, supervision, project administration, funding acquisition.

Publisher's Disclaimer: This is a PDF file of an unedited manuscript that has been accepted for publication. As a service to our customers we are providing this early version of the manuscript. The manuscript will undergo copyediting, typesetting, and review of the resulting proof before it is published in its final form. Please note that during the production process errors may be discovered which could affect the content, and all legal disclaimers that apply to the journal pertain.

Author Manuscript Author Manuscript Author Manuscript Author Manuscript

in adjacent surrounding cells only in C5a-treated monolayers. These results suggest that C5a/C5aR signaling produced an intermediate state, characterized by increased mitochondrial fusion and ER-mitochondrial contacts, that sensitizes cells to oxidative stress, leading to mitochondrial fragmentation and cell death. s

Graphical Abstract

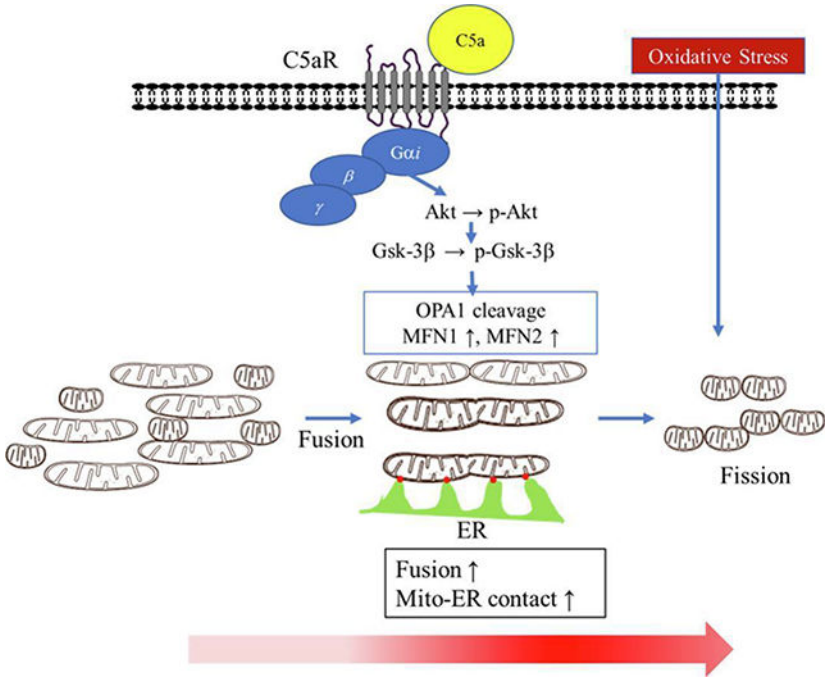

C5a/C5aR signaling induced mitochondrial fusion and increased ER-mitochondrial contacts to sensitize against oxidative stress to trigger mitochondrial fission. Under baseline conditions, C5a-C5aR-Gαi signaling induces mitochondrial fusion together with an increase in mitochondrial-ER contact sites, involving an increase in the expression of the mitochondrial fusion-proteins, MFN1, MTF2 and OPA1, and the promotion of OPA1 cleavage. The C5aR-mitochondria signaling cascade includes PI3K activation and Akt phosphorylation [45], followed by Gsk-3β phosphorylation at Ser9. Increased mitochondrial fusion sensitizes the mitochondrial network to a secondary stressor, such that C5a-treatment in the presence of oxidative resulted in excessive mitochondrial fission, ultimately leading to cell death. Abbreviations: Akt, protein kinase B; C5a, complement component 5a; C5aR, complement C5a receptor; ER, endoplasmic reticulum; MFN1, mitofusin-1; MFN-1, mitofusin-2; OPA1, optic atrophy 1; p-Akt, phosphorylated Akt; PI3K, phosphoinositide 3-kinase.

Keywords

anaphylatoxin; G-protein coupled receptor; mitochondrial dynamics; ER-mitochondria contact

Author Manuscript Author Manuscript Author Manuscript Author Manuscript

Introduction

The complement system is an essential part of the immune system involved in eliminating foreign antigens and pathogens as part of the normal host defense response [1]. The complement system is activated by various stimuli, such as oxidative stress, inflammatory factors, and ischemia [2]. Depending on the pathogen-associated molecular patterns (PAMPs) or damage-associated molecular patterns (DAMPs), the complement system can activate three distinct pathways: the classical pathway (CP), lectin pathway (LP), and alternative pathway (AP). The three pathways all participate in forming C3 convertases that will catalyze the proteolytic cleavage of complement component 3 (C3) into C3a and C3b. C3b subsequently participates in the formation of C5 convertases that cleave complement component 5 (C5) into C5a and C5b. As the final step of the complement cascade, C5b initiates the formation of the membrane attack complex (MAC) on membranes together with C6, C7, C8, and C9 to promote sublytic cell signaling or cell lysis [1]. The anaphylatoxins C3a and C5a have multiple roles in vasodilation and enhancing vascular permeability, as well as the mediation of chemotaxis and inflammation and the generation of cytotoxic oxygen radicals, which are mediated by their receptors C3a-, C5a-, and C5a-like receptor 2 (C3aR, C5aR, and C5L2) [2]. C3aR, C5aR, and C5L2 are members of the G-protein-coupled receptor (GPCR) families. C5aR is expressed widely on many cell types, but has mostly been studied in cells of myeloid origin, including monocyte/macrophages and microglia. Additionally, C5aR is expressed on endothelial and epithelial cells in tissues including the lung, liver, kidney, and brain [2].

The mitochondrion is an organelle that plays an essential role in producing bioenergetic adenosine triphosphate (ATP) through the respiratory metabolism process of oxidative phosphorylation (OXPHOS). Also, mitochondria regulate cell fate by releasing cell death signaling activating caspase activity, through an event of mitochondrial outer membrane permeabilization (MOMP), responding to extra- and intra-mitochondrial changes and signaling [3]. Mitochondrial network morphology represents the cellular status of respiration and damage. Mitochondrial morphology is a dynamic change and a balance between fission and fusion. The ratio between lengthened and fragmented mitochondria is altered flexibly, responding to mitochondrial metabolic status and extra-mitochondrial signaling. Specifically, mitochondrial morphology is regulated with intracellular signaling linked to GTPase-dynamin-related proteins.

Regarding complement signaling and mitochondrial function, we previously reported that mitochondria in mouse retinal pigment epithelial (RPE) cells *in vivo* are localized at a higher density along the basal rather than the apical side. However, AP activation triggered with long-term passive inhalation of cigarette smoke perturbed that gradient and increased mitochondrial size [4]. More recently, we reported that plasma membrane C3aR was found to be transported to mitochondria (mtC3aR) in response to oxidative stress induced by H_2O_2 treatment; and mtC3aR activation enhanced mitochondrial Ca^{2+} uptake and inhibited mitochondrial electron transport chain activities, resulting in reduced state III-ATP production and maximal respiratory capacity in isolated mitochondria [5].

Author Manuscript Author Manuscript Author Manuscript Author Manuscript

C5aR activation has been shown to enhance protein kinase B (Akt) phosphorylation via phosphatidylinositol-3-kinase (PI3K) in ARPE-19 cells [6] and in neutrophils [7]. Also, C5aR activation enhanced Gsk-3β phosphorylation via Akt phosphorylation on platelet [8]; and, C5a-treatment induced an inhibition of oxygen consumption in PC12 cells, increased mitochondrial stress, and reduced cell growth [9]. Further, C5aR-deficiency in mice altered oxygen consumption if exposed to a high fat or high sucrose diet [10]. However, to date it is unclear how C5a/C5aR signaling might alter the physiological phenotype of mitochondria.

In the present study, we addressed the overall question of whether C5a/C5aR signaling enhances and/or protects cells from cellular damage. Specifically, we investigated C5a/C5aR signaling associated with mitochondrial dynamics, and the effects of oxidative stress in that process. Surprisingly, we found that C5aR activation induced mitochondrial fusion, increased mitochondrial fusion-related protein levels, and increased the mitochondrial-endoplasmic reticulum (ER) contact frequency in ARPE-19 cells grown as polarized cells. However, exogenous oxidative stress in C5a-treated cells promoted the formation of pyknotic nuclei and enhanced mitochondrial fragmentation. Likewise, endogenous oxidative stress produced by blue laser spot stimulation of a single cell within an ARPE-19 monolayer induced mitochondrial fragmentation in their neighboring cells faster in C5a- when compared to the untreated monolayers. These results suggested that mitochondrial fusion and increased levels of ER-mitochondrial contacts induced by C5aR activation represent an intermediate state between healthy (partially fused) and fission, with increased fission ultimately leading to cell death. These studies will have significant implications in epithelial cell biology and the future development of anti-complement therapeutics.

Materials and Methods

Cells

ARPE-19 cells (immortalized human RPE cells, passage 22–40; ATCC, Manassas, VA), expanded in DMEM including 10% fetal bovine serum (FBS) with 1% antibiotic–antifungal (AA) agents (Thermo Fisher, Waltham, MA), were chosen, as, when grown as monolayers, they express many of the signature genes of primary human RPE cells, develop tight, adherence and gap junctions, and resemble an aged RPE phenotype over time [11].

Preparation of cells for imaging or immunocytochemistry.

ARPE-19 cells were dissociated with Trypsin-EDTA, plated on 35 mm glass-bottom dishes (MatTek, Ashland, MA) and matured for 2 weeks in DMEM (with phenol red) and 1 % AA, containing 1% FBS to enable the development of tight junctions. Culture medium was changed to phenol-red and FBS free DMEM containing 1 mM HEPES (pH 7.4) 3 hour prior to imaging. Cells were labeled with the following fluorescence dyes: 0.5 μM MitoTracker Deep Red (MTDR; Molecular Probes, Eugene, OR) to detect mitochondria; 4 μM ER-Tracker Green (ERTG; Molecular Probes, Eugene, OR) to identify the endoplasmic reticulum (ER), and 1 mM Hoechst33342 (Thermo Fisher, Waltham, MA) to label the nuclei. Labeling was performed in phenol-free DMEM (Invitrogen, Waltham, MA) containing 1 mM 4-(2-hydroxyethyl)-1-piperazineethanesulfonic acid (HEPES) and buffered to pH 7.4. In some monolayers, a highly specific full antagonist of the C5aR

Author Manuscript Author Manuscript Author Manuscript Author Manuscript

(W-54011, 100 nM; Millipore-Sigma, Burlington, MA, PMID: 12384495, [12]), 100 nM Tat-GPR (G-protein αi inhibitor, kindly provided by Yuri Peterson, MUSC, [13]), 10 μM 3F8 (Gsk-3β inhibitor, R&D Systems, Minneapolis, MN, [14]) were added to culture medium 2 hours before imaging. C5a peptide at 52 nM (Complement Technology, Tyler, TX [15]) was added to the culture medium at 1 hour before imaging.

Immunocytochemistry

Immunocytochemistry was performed on cells grown for >2 weeks post confluency on glass bottom dishes and glass bottom 96-well microplates (Mattek, Ashland, MA). Cells were labeled with MTDR, ERTG and Hoechst33342 prior to fixation. For immunolabeling, monolayers were fixed with 4% paraformaldehyde in 0.1 M phosphate buffer for 30 minutes. To block the nonspecific immunoreactivity, 30% Bovine Serum Albumin (BSA) and 1% Normal Goat Serum (NGS) in 0.1 M PBS was used. Antibodies in this paper were listed in Table 1. Primary antibodies included a specific antibody against C5aR (1:1000), anti-Mitofusion-1, and −2 (1:300). Alexa Fluor 488 anti-rabbit IgG secondary antibody was used at 1:200.

Western Blotting

ARPE-19 cells were homogenized in radioimmunoprecipitation assay buffer (RIPA, 5 M sodium chloride, 1 M Tris-HCl, 1 % Nonidet P-40, 10 % SDS) supplemented with protease inhibitor cocktail, and 10 mM phenylmethylsulfonyl fluoride (Sigma-Aldrich, St. Louis, MO). The homogenates were centrifuged (800 × g for 10 min) to separate nuclei and supernatant to eliminate nuclear proteins. 30 μg proteins measured by NanoDrop (Thermo Scientific, Waltham, MA) were loaded per well. Following separation, the protein was transferred to PVDF membranes (iBlot system; Invitrogen, Waltham, MA) and probed with antibodies (see Table I) at 1:1000, followed by HRP-conjugated secondary IgG antibodies (Cell Signaling, Danvers, MA). Chemiluminescent substrate for HRP (Pierce ECL Western Blotting Substrate; Thermo Scientific, Waltham, MA) was used, and the chemiluminescent signals captured with ImageQuant LAS 4000 Gel Imaging System (GE Healthcare Bio-Sciences, Pittsburgh PA). After capturing the immunoreactive band, the membranes were treated with ReBlot medium (Millipore-Sigma, Burlington, MA) for 10 minutes and re-probed for β-actin. The intensity of the specific bands was measured with ImageJ software (NIH, Bethesda, MD).

Confocal imaging

We have previously reported the method for live cell imaging of ARPE-19 monolayers grown on a 35 mm glass-bottom dishes (Mattek) [16]. The monolayers were prepared as described above (Preparation of cells for imaging or immunocytochemistry). Fluorescence images of mitochondrial dynamics and live cell imaging were captured with a spinning-disk confocal microscope (Ultraview, Perkin Elmer, Waltham, MA) with a Nikon Ti microscope (Tokyo, Japan) controlled by the Volocity Imaging software (Perkin Elmer, Waltham, MA) on the Dell Workstation computer as published [5]. Fluorescence images captured by z-stack (0.2 μm per slice) tracked signals from the basal to the apical surface, collecting images with a ×40 (apoptosis) and a ×60 lens (all other imaging). For image acquisition, and to prevent artifacts based on repeated laser excitation during image acquisition, laser power was set

Author Manuscript Author Manuscript Author Manuscript Author Manuscript

at a maximum intensity of 0.5% for the 488, and 640 nm laser lines (all at 50 mW raw laser power). Likewise, the duration of laser excitation during image acquisition was set at 200 ms to prevent sampling bias and retain good image contrast. Under these conditions, long-term imaging did not induce photo-oxidative stress (i.e., no alternations in ROS levels as determined by CRG) or changes in mitochondrial membrane potential (as determined by TMRM).

Blue laser stimulation

488 nm spot laser stimulation on a single ARPE-19 cell within a cellular network, which induced a bystander effect in neighboring cells, was previously reported by us [16]. Specifically, a single cell was stimulated repeatedly within the location of the mitochondrial network with a blue spot laser (488 nm, spot size setting of 'small circle', 0.32 μm diameter) using the built-in photo-bleaching device of the Ultraview VoX system, using a 20 ms, 10-cycle pulse stimulation every 1 s (1 Hz) at 10% laser intensity (38 kw/cm^2). These parameters have been shown by us previously to result in reproducible effects on ROS and mitochondrial membrane potential, triggering a response in both the stimulated (primary) followed by connected (secondary, tertiary and quaternary) cells [16].

Data analysis

Mitochondrial morphology, focusing on mitochondrial length (mean and median), number of branches per mitochondrion, and overall footprint was analyzed quantitatively by MiNA (Mitochondrial Network Analysis) plugin [17] in Fiji software (NIH, Bethesda, MD). The data was analyzed with GraphPad Prism (GraphPad Software, Inc.) and SPSS (IBM), and statistical significance was determined with Student's t-test, parametric One-way ANOVA, Nonparametric Mann-Whitney U-test and Kruskal-Wallis test, and presented as $p < 0.05$, 0.01, 0.001. 0.0001.

Antibodies

Antibodies for immunolabeling and western blotting in this study are listed (Table I).

Results

C5aR activation induced mitochondrial fusion

We have previously reported C5 and C5aR mRNA and protein expression in ARPE-19 cells [6]. First, we followed up this observation to confirm the presence of C5aR protein in fully differentiated ARPE-19 cell monolayers by Western blot analysis (Figure S1) and immunolabeling. First, we confirmed antibody specificity with Western blot analysis. The antibody recognized a band of ~43 kDa, the expected molecular weight of C5aR [18], which was reproduced in cellular protein samples from three different culture dishes (Figure S1). C5aR-Alexa Fluor 488 immunoreactive particles (green) were identified on the WGA-labeled plasma membrane in 3D-images reconstructed from acquired z-stacks (0.2 μm/image slice) (Figure 1A) and the orthogonal, confirming their presence in clusters on the apical membrane (red, colocalization identified as yellow particles) (Figure B).

Author Manuscript Author Manuscript Author Manuscript Author Manuscript

Also, We previously reported that 52 nM C5a polypeptide activated C5aR-Akt signaling and resulted in the elevation of intracellular calcium [6]. Here we adopted the same C5a concentration of 52 nM throughout the experiments in this study. Surprisingly, confocal microscopy for MTDR mitochondria-related fluorescence demonstrated that 52 nM C5a-treatment induced mitochondrial fusion (Figure 1C, second panel) compared with the no-treatment control (Figure 1C, first panel). While oxidative stress triggered by the exposure of cells to 0.5 mM H_2O_2 triggered mitochondrial fragmentation when compared to control, H_2O_2-exposure following C5a-treatment resulted in mitochondrial fragmentation in a dose-dependent manner (Figure 1D), resulting in maximal fragmentation at 0.5 mM H_2O_2 (Figure 1C, panel 3). The mitochondrial networks were analyzed using the MiNA plugin on Fiji/ImageJ software to quantify mean branch length, median branch length and the number of branches of individual mitochondria (Figure 1D). Specifically, this analysis indicated that mean mitochondrial branch length (Figure 1D, left panel) was 50% longer in C5a-treatment than in controls (C5a-treatment 2.03±0.21 μm, control 1.51±0.15 μm mean±stdev, **p< 0.01). Exposure of the cells to C5aR-antagonist prior to C5a-treatment prevented the elongation compared with the C5a-treatment (****p<0.0001). Interestingly, 0.2 mM H_2O_2 treatment on C5a-pretreated ARPE-19 cells inhibited the C5a-induced mitochondrial elongation close to the untreated controls, whereas 0.5 mM H_2O_2 treatment induced mitochondrial hyperfragmentation. Median mitochondrial branch length (Figure 1D, middle panel) was affected the same way. Mitochondrial branch analysis or branching of individual organelles (Figure 1D, right hand panel) demonstrated that the C5a-treatment alone as well as 0.5 mM H_2O_2-treatment prior to C5a-treatment reduced mitochondrial network complexity when compared to the controls, 0.2 mM H_2O_2-treatment, and C5aR-antagonist pre-treatments.

C5aR activation increased mitochondrial fusion proteins and signaling

Intracellular signaling and dynamin-like GTPase proteins, OPA1, MFN1, and MFN2 regulate mitochondrial dynamics by increasing fusion whereas Drp1 controls fission. OPA1 is associated with the inner mitochondrial membrane (IMM), with OPA1 cleavage to long- (l-OPA1) and short-chain (s-OPA1) being required for the fusion event. MFN1 and MFN2, on the other hand, are required for outer mitochondrial membrane (OMM) fusion. Thus, we further tested whether C5a-treatment affected the mitochondrial fusion protein levels using Western blot analysis. ARPE-19 protein was collected 1 hour after C5a treatment. Western blot analysis demonstrated that total OPA1 protein of s- and l-OPA1 in C5a-treated cells was elevated by 1.7-fold when compared to the control cells (*p<0.01), as were s-OPA1 (2-fold; **p<0.01) and l-OPA1 (1.5-fold; **p<0.01) (Figure 2A). The critical s-OPA1/l-OPA1 ratio was also elevated by 1.6-fold when compared to controls (**p<0.01). Furthermore, MFN1 protein showed a 1.7-fold (*p<0.05), MFN2 a 1.25-fold higher (**p<0.01) expression level when compared to the control.

Mitochondrial fusion can occur in the presence or absence of changes in the pro-fission protein Drp1 [19]. However, Drp1-deficiency has been shown to induce mitochondrial fusion [20]; and mdivi1, an inhibitor of Drp1, inhibited mitochondrial fragmentation in H_2O_2-treated, subconfluent ARPE-19 cells [21]. Tyrosine phosphorylation of Erk1/2 at Thr202 and Tyr204 mediated by MAPK activation, leads to phosphorylation of Drp1

Author Manuscript Author Manuscript Author Manuscript Author Manuscript

at Ser616, which has been reported to enhance mitochondrial fragmentation. Thus, we tested whether C5a-treatment inhibited p-Erk1/2 and p-Drp1 levels using Western Blotting analysis. However, C5a application to activate C5aR signaling did not change p-Erk1/2 (Thr202/Tyr204) or p-Drp1 (Ser616) levels (Figure 2B).

Next in the cascade, since C5aR activation on mouse platelet enhances Gsk-3β phosphorylation [8], and Akt-Gsk-3β signaling enhances OPA1 cleavage and mitochondrial fusion in osteoblast cells [22], we tested whether C5aR activation altered p-Gsk-3β level in ARPE-19 cells with Western blot analysis. The p-Gsk-3β (Ser9)/Gsk-3β ratio upon C5a-treatment was elevated 2.5-fold when compared to controls, and C5aR-antagonist treatment prior to C5a-treatment inhibited the increase (Figure 2C). To confirm that Gsk-3β phosphorylation contributes to mitochondrial fusion induced by C5a-treatment, we tested whether Gsk-3β inhibition using 3F8 (1 μM) treatment prior to C5a-exposure affected mitochondrial fusion. 3F8 inhibited C5a-induced mitochondrial branch length elongation both at mean (*$p< 0.05$) and median comparisons (*$p<0.05$) (Figure 3). Furthermore, we tested Gai-specific inhibitor Tat-GPR [13]to confirm the C5aR- G-protein associated signaling effecting on C5a-induced mitochondrial elongation. Tat-GPR pre-treatment inhibited C5a-induced mitochondrial elongation in mean and median, the level was same as the control (Figure 3).

Mitochondrial fusion in response to C5a is not affected by mitochondrial redox status.

Severe oxidative stress has been shown to induce mitochondrial fragmentation, ultimately promoting the release of cell death signals such as cytochrome c, leading to apoptosis. However, lower oxidative stress enhances mitochondrial elongation and inhibits mitochondrial fission by inhibition of Drp1 [23]; and mitochondrial elongation is assumed to be a protective mechanism to dilute mitochondrial ROS [24]. Therefore, we tested whether mitochondrial fusion induced with C5a treatment depended on mitochondrial ROS. To monitor ROS, CellRox Green was utilized, which detects ROS in the form of superoxide anions and hydroxyl radicals in mitochondria [25]. C5a-treatment increased CellRox Green fluorescence, particularly in mitochondria, and NAC treatment prior to C5a exposure inhibited the fluorescence increase (Figure 4A, B). However, NAC did not affect C5a-induced mitochondrial fusion and mean mitochondrial branch length (Figure 4A, B). This result suggests that C5a-induced mitochondrial fusion is independent of mitochondrial ROS levels.

C5a-treatment sensitized the mitochondrial network against oxidative stress.

Following the results of C5a-induced mitochondrial fusion, we addressed the question whether mitochondrial fusion is overall protective or sensitizes the cell to cell death when exposed to a second stressor. Thus, we tested whether C5a-treatment promoted cell death in oxidatively stressed ARPE-19 cell monolayers using confocal microscopy. The formation of pyknotic nuclei was monitored over a four-hour period, using Topro-3 [26]. Nucleus status were categorized to 3 status, viable (weak, arrow), early (intermediate, yellow arrowhead), and late apoptotic pyknosis (solid red arrowhead) by Topro-3 fluorescencce intensity corelating nucleus shapes (Figure S2). Untreated controls, cells treated with C5a alone, or those exposed to 0.5 mM H_2O_2 showed little change in the number of pyknotic

Author Manuscript Author Manuscript Author Manuscript Author Manuscript

nuclei over the observation period (Figure 5A, B). However, C5a-exposure followed by 0.5 mM H_2O_2-treatment increased the number of early and late pyknotic nucleus over the four hour period to 40 %, late pyknotic nucleus were increased to 30% of total nucleus (Figure 5 A, B). These results suggest that the C5a-treatment sensitized the cells to H_2O_2, ultimately leading to cell death. Furthermore, the C5a-induced cell death sensitization might be associated with mitochondrial calcium level, we tested mitochondrial calcium uniporter blocker Ru360. Ru360 pre-treatment folloing by C5a and H_2O_2 treatment inhibited nucleus pyknotic change (Figure 5 A, B).

C5aR activation increased the number of ER-mitochondrial contacts

MFN2 is distributed not only on the OMM but also on the ER membrane and plays a crucial role in ER-mitochondrial contact formation. Following up on the results that C5aR activation increased mitochondrial elongation and elevated intracellular MFN2 levels (Figures 1, 2), we hypothesized that C5a-treatment might enhance mitochondrial elongation to promote ER-mitochondrial contact formation. Thus, we tested whether C5a-treatment increased the frequency of ER-mitochondrial contacts in C5a-treated ARPE-19 monolayers. ER was labeled with ERTG (green, Figure 6A), and mitochondria with MTDR (magenta) 30 minutes before adding 52 nM C5a. After addition of C5a-peptide, the cells were fixed with 4% PFA for 15 minutes in intervals of 30 minutes, up to 2 hours. Monolayers were imaged by confocal microscopy, assaying for colocalization of the two signals (white). In short, the 3D-ERTG and MTDR network images were converted to skeleton images with the skeleton 3D plugin, followed by the application of the colocalization plugin, and the quantification of the colocalized dots (Fiji/ImageJ, Figure 6B). The number of ER-mitochondrial contact sites did not change over the 2 hour observation period in untreated cells (control) (Figure 6C). In contrast, C5a-treatment increased the number of ER-mitochondria contacts by 200% at 120 minutes, or the end of the observation period (***$p<0.001$) (Figure 6C). C5aR-antagonist pretreatment prior to the exposure to C5a prevented the increase in contact sites (Figure 6C).

C5aR activation enabled a bystander effect, triggering mitochondrial fragmentation in neighboring cells.

Thus far we have investigated the effects of C5aR activation in the presence of oxidative stress throughout the entire RPE network. We previously reported blue laser spot stimulation on a single cell of ARPE-19 cell within a monolayer as a method to induce local oxidative stress. And importantly, this locally induced oxidative stress triggered a bystander effect mediated by H_2O_2 and Ca^{2+}, spreading from the stimulated to the adjacent surrounding cells [27]. Here, as the final experiment of this study, we tested whether photo-oxidative stress induces mitochondrial fission in the stimulated (false colored in red) and neighboring cells, and whether C5a-pretreatment enhances either one of those effects. Mitochondrial network dynamics were analyzed in MTDR-stained cells and determined for the direct neighbors of the stimulated cell (primary neighbors; false colored in green) and those surrounding the primary cells (secondary neighbors; false colored in white). Blue laser spot stimulation on a single cell induced mitochondrial fragmentation and ultimately destroyed the stimulated cell over the 10-minute recording period in control, C5a-treated, and C5aR-antagonist and C5a-treated cells (Figure 7A). At time point zero, as expected, the mitochondrial network exhibited greater fusion (branch length) in the C5a treated cells when

Author Manuscript Author Manuscript Author Manuscript Author Manuscript

compared to controls. Interestingly, mitochondrial fragmentation was seen in the primary adjacent cells in C5a-treated cultures (green) as early as the 2 minute timepoint, and in the secondary cells by 6 minutes. Overall, mitochondrial length was reduced to almost half by minute 10, or the end of the stimulation and recording period (middle panels in Figure 7A). In contrast, mitochondrial fragmentation on the primary and the secondary adjacent cells in untreated control cells did not show any obvious changes (upper panels in Figure 7A). C5aR-antagonist treatment prior to C5a-exposure prevented the bystander effect (lower panels in Figure 7A). Quantitative analysis with MiNa plugin in Fiji/ImageJ to examine the mitochondrial length changes supported the visual images. In C5a-treated cell, the mean mitochondrial length of the primary adjacent cells was shortened by the 2nd minute (***$p<0.001$) and continued shortening to end of the experiment in comparison with the control cells (***$p<0.001$) (Figure 7B). Likewise, in the secondary cells of the C5a-treated monolayer, mitochondrial length was shortened by the 6th minute (***$p<0.001$) and continued shortening to the 10th minute (***$p<0.001$) (Figure 7B). Effects on both primary and secondary cell mitochondrial fission was prevented by C5aR-antagonist pretreatment prior to C5a exposure (Figure 7B).

Discussion

Here we set out to further contribute to the analysis of complement signaling in epithelial cells and assess effect of anaphylatoxin receptor signaling in regulating cellular damage associated with mitochondria. Our key findings in this study were: 1. C5aR activation regulated mitochondrial dynamics and induced fusion events in resting cells; 2. the C5a/C5aR signaling axis increased mitochondrial fusion-related proteins MFN1 and MFN2, and induced OPA1 cleavage required for mitochondrial fusion events; 3. mitochondrial fusion induced by C5aR activation was independent of mitochondrial ROS levels; 4. C5aR-activation enhances Gsk-3β-phosphorylation at Serine 9; 5. C5aR activation increased the number of mitochondria-ER contact sites; 6. treatment of cells with C5a prior to H_2O_2 exposure enhanced mitochondrial fragmentation and promoted nuclear pyknosis; 6. Induction of oxidative stress in a single cell using spot blue laser stimulation induced a bystander effect of mitochondrial fragmentation in adjacent surrounding cells only in the presence of C5a (see Graphical Abstract).

In many diseases of barrier dysfunction, the cells are exposed to complement and oxidative stress [28]. Our results suggest that in cells exposed to both C5a/C5aR stimulation and oxidative stress, C5a produces an intermediate state characterized by mitochondrial fusion and ER-mitochondrial contacts which then sensitizes the cells to oxidative stress, leading to mitochondrial fragmentation and cell death.

C5a/C5aR – G-protein signaling to induce mitochondrial fusion.

The C5a receptor is a seven transmembrane receptor coupled with G-proteins that are associated with two distinct Gα subunits: Gαi, which is pertussis toxin (PTX) sensitive, and the PTX-insensitive Gα15 (Gα16 in humans) [29, 30]. There are previous reports of GPCR-activity affecting mitochondrial dynamics such as those involving the β2-adrenergic receptor and the P2YR2 purinoceptor. Specifically, activating β2-adrenergic receptor-Gαi

Author Manuscript Author Manuscript Author Manuscript Author Manuscript

signaling promoted mitochondrial fusion in mouse skeletal muscle [31]. In contrast, $P2YR_2$ purinoceptor-Gαs signaling induced mitochondrial fission in ischemic brain tissue [32]. However, the exact pathway by which Gαi or Gαs signaling led to mitochondrial fusion and fission, respectively, was not investigated by the authors.

In our results, we showed that C5a/C5a-Gαi signaling induced mitochondrial fusion and increased the amount of mitochondrial fusion proteins MFN1 and MFN2 as well as OPA-1 cleavage. The C5aR-antagonist, as well as the Gαi-specific inhibitor Tat-GPR, inhibited mitochondrial fusion induced by C5aR activation. We previously reported that C5aR activation enhance PI3K phosphorylation following by protein kinase B (Akt) phosphorylation [6]. Therefore, these results strongly suggested that C5a/C5aR, followed by PI3K-Akt signaling provide the link to mitochondrial fusion. Important to note in this context, p-Akt has been shown to activate Bcl-2, which inhibits the release of cell death signaling molecules from mitochondria, promoting cell survival [6, 33].

To complete the signaling pathway from C5aR activation to mitochondrial fission/fusion, we explored other known activators in the PI3K-Akt signaling pathway. C5aR activation has been shown to enhance Akt phosphorylation [6], while p-Akt enhances Gsk-3β phosphorylation [34]. Phosphorylated-Gsk-3β (p-Gsk-3β) at serine 9 is known to interact with the mitochondrial fission protein Drp1, regulating mitochondrial motility [35]. Also, Gsk-3β in mitochondria (mtGsk-3β) has been shown to regulate the mitochondrial permeable transition pore (mPTP) opening via cyclophilin-D, assumed to prevent mitochondrial calcium overload in mitochondria and thereby promoting cell survival [36]. In contrast, Akt-Gsk-3β signaling has been shown to enhance fusion, and phosphorylated Gsk-3β has been shown to promote OPA1 cleavage and mitochondrial fusion in murine osteoblast MC3T3-E1 cells [22]. Interestingly, Gsk-3β has been reported to be distributed on ER-mitochondria contact sites where it was involved in regulating 1,4,5-trisphosphate (IP3) receptors (IP3R) and mediated calcium release from mitochondria in myocardiac cells in ischemia-reperfusion injury [37]. Our results demonstrated that Gsk-3β-inhibition inhibited C5a-induced mitochondrial fusion in resting RPE monolayers. Thus, Gsk-3β regulation of mitochondrial dynamics might be associated with multiple signaling cascades and crosstalk, depending on whether the mechanisms are investigated in a disease model or in naïve cells.

C5aR activation has also been shown to enhance signaling, involving p38/MAPK activity and Erk1/2 phosphorylation. This mechanism is involved in upregulating protein expression of inflammatory factors, interleukin-6 (IL-6), and tumor necrosis factor-α (TNF-α) in primary cultures of mouse microglial cells [38]. In confluent cultures of ARPE-19 cells, C5a stimulated the production of TLR-4-induced IL-6 or IL-8, which required phosphorylated Erk1/2 but not p38/MAPK activity [12]. However, the C5aR activation mediated Erk1/2 phosphorylation at Ser543 in ARPE-19 only in the presence of lipopolysaccharide (LPS) treatment, a severe proinflammatory state [12]. Here we showed that C5aR activation in naïve ARPE-19 did not affect MAPK/Erk1/2 signaling, nor did it increase Erk1/2-mediated phosphorylation on Drp1 at Serine 9. Indeed, C5aR activation did not induce any change in Erk1/2 phosphorylation. Thus, as with Gsk-3β regulation, the involvement of Erk1/2-mediated signaling also seem to depend on whether the mechanism is investigated in a disease model or in naïve cells.

Author Manuscript Author Manuscript Author Manuscript Author Manuscript

C5aR activation increased ER-mitochondrial contacts

MFN2 is distributed not only on OMM but also on the ER membrane and plays a crucial role in ER membrane tethering to mitochondria [39]. Overall, ER-mitochondrial contacts are thought to facilitate calcium homeostasis, phospholipid transfer to mitochondria that are synthesized within the ER, promote mitochondrial fission at the contact sites and ultimately trigger apoptosis by increasing calcium transfer and release of cytochrome c from the mitochondria [40]. In Western Blots, both MFN1and MFN2 protein levels were increased by C5a-treatment. In addition, C5a-treatment induced mean and median mitochondrial branch elongation,reduced the number of network branches and increased ER-mitochondrial contact sites. These results suggested that C5a-induced mitochondrial fusion might promote the formation of ER-mitochondria contacts. Further, we obtained a result that exogenous H_2O_2 treatment on C5a-pretreated ARPE-19 cells enhanced mitochondrial fission and resulted in the formation of pyknotic nuclei, leading to cell death (Figure 3). The formation of pyknotic nuclei could be completely inhibited by pretreatment with the mitochondrial calcium uniporter blocker, Ru360, which demonstrated that calcium transfer from ER to mitochondrial at ER-mitochondrial contact sites is involved in C5a+H_2O_2 mediated cell death. Taken together, our results suggest that increasing ER-mitochondrial contact frequency by C5aR activation contributes to enhanced mitochondrial fission in the presence of oxidative stress generated by H_2O_2 exposure or by the generation of endogenous H_2O_2 produced by blue laser spot stimulation.

Summary

Here we tested the question whether complement activation via the C5a receptor together with oxidative stress modulates mitochondrial dynamics. In aging and many diseases, oxidation-inflammation are the underlying causes of impairment of function. And mitochondria are not only the source of reactive oxygen species, but they are the integrators of the cell's metabolic status and cellular damage, and ultimately the decision makers over cell survival or cell death. We analyzed retinal pigment epithelial cells, which in the eye are part of the blood retina barrier, and part of the innate immune system that separates the neural retina from the blood stream and potentially damaging components. These cells express many complement components [41], are the target of complement activation [42], exhibit impaired mitochondrial function and oxidative stress with aging [43], and undergo excessive mitochondrial fission with aging and disease [44]. We showed that in a human RPE cell line, C5aR activation induced mitochondrial fusion and increased ER-mitochondrial contact frequency. In the context of oxidative stress, whether delivered exogenously via H_2O_2 exposure, or endogenously via blue light stimulation of the mitochondrial network [16] C5a-mediated fusion promoted excessive mitochondrial fission, ultimately leading to cell death. These results suggest that mitochondrial fusion induced by C5aR activation shifted the mitochondrial physiological status to an intermediate status; and when exposed to a secondary damaging stimulus, accelerated mitochondrial fission, that could lead to cell death. Thus, in the context of aging and disease, mitochondrial fusion triggered by C5aR activation might be an early protective response to potentially dilute ROS or mix damaged and normal DNA; but in the context of excessive ROS accumulation, C5aR activation tips the balance towards mitochondrial fission. Hence, the

Author Manuscript Author Manuscript Author Manuscript Author Manuscript

analysis of C5aR activation and components of the C5aR signaling axis might provide clues to novel therapeutic approaches in complement-dependent diseases such as age-related macular degeneration and other diseases involving barrier epithelial cells, many of which are complement signaling-related human diseases.

Supplementary Material

Refer to Web version on PubMed Central for supplementary material.

ACKNOWLEDGMENTS

Funding for this project was provided in part by the National Institutes of Health (NIH) R01EY030072, the Department of Veterans Affairs IK6 BX004858, RX000444 and BX003050, and the South Carolina SmartState Endowment. We would like to acknowledge Yuri Peterson (Department of Drug Discovery and Biomedical Sciences, MUSC) for his generous gift of Tat-GPR, and Christin Edge (Department of Ophthalmology, MUSC) for editorial assistance.

References

[1]. Muller-Eberhard HJ, Molecular organization and function of the complement system, Annu Rev Biochem 57 (1988) 321–47. [PubMed: 3052276]

[2]. Klos A, Tenner AJ, Johswich KO, Ager RR, Reis ES, Kohl J, The role of the anaphylatoxins in health and disease, Mol Immunol 46(14) (2009) 2753–66. [PubMed: 19477527]

[3]. Osellame LD, Blacker TS, Duchen MR, Cellular and molecular mechanisms of mitochondrial function, Best Pract Res Clin Endocrinol Metab 26(6) (2012) 711–23. [PubMed: 23168274]

[4]. Woodell A, Coughlin B, Kunchithapautham K, Casey S, Williamson T, Ferrell WD, Atkinson C, Jones BW, Rohrer B, Alternative complement pathway deficiency ameliorates chronic smoke-induced functional and morphological ocular injury, PLoS One 8(6) (2013) e67894. [PubMed: 23825688]

[5]. Ishii M, Beeson G, Beeson C, Rohrer B, Mitochondrial C3a Receptor Activation in Oxidatively Stressed Epithelial Cells Reduces Mitochondrial Respiration and Metabolism, Front Immunol 12 (2021) 628062. [PubMed: 33746964]

[6]. Busch C, Annamalai B, Abdusalamova K, Reichhart N, Huber C, Lin Y, Jo EAH, Zipfel PF, Skerka C, Wildner G, Diedrichs-Mohring M, Rohrer B, Strauss O, Anaphylatoxins Activate Ca(2+), Akt/PI3-Kinase, and FOXO1/FoxP3 in the Retinal Pigment Epithelium, Front Immunol 8 (2017) 703. [PubMed: 28663750]

[7]. Wrann CD, Tabriz NA, Barkhausen T, Klos A, van Griensven M, Pape HC, Kendoff DO, Guo R, Ward PA, Krettek C, Riedemann NC, The phosphatidylinositol 3-kinase signaling pathway exerts protective effects during sepsis by controlling C5a-mediated activation of innate immune functions, J Immunol 178(9) (2007) 5940–8. [PubMed: 17442978]

[8]. Nording H, Baron L, Haberthür D, Emschermann F, Mezger M, Sauter M, Sauter R, Patzelt J, Knoepp K, Nording A, Meusel M, Meyer-Saraei R, Hlushchuk R, Sedding D, Borst O, Eitel I, Karsten CM, Feil R, Pichler B, Erdmann J, Verschoor A, Chavakis E, Chavakis T, von Hundelshausen P, Köhl J, Gawaz M, Langer HF, The C5a/C5a receptor 1 axis controls tissue neovascularization through CXCL4 release from platelets, Nat Commun 12(1) (2021) 3352. [PubMed: 34099640]

[9]. Martinus RD, Cook CJ, The effect of complement C5a on mitochondrial functions of PC12 cells, Neuroreport 22(12) (2011) `581–5. [PubMed: 21734613]

[10]. Roy C, Gupta A, Fisette A, Lapointe M, Poursharifi P, Richard D, Lu H, Lu B, Gerard N, Gerard C, Cianflone K, C5a receptor deficiency alters energy utilization and fat storage, PLoS One 8(5) (2013) e62531. [PubMed: 23667486]

[11]. Ablonczy Z, Dahrouj M, Tang PH, Liu Y, Sambamurti K, Marmorstein AD, Crosson CE, Human retinal pigment epithelium cells as functional models for the RPE in vivo, Invest Ophthalmol Vis Sci 52(12) (2011) 8614–20. [PubMed: 21960553]

Author Manuscript Author Manuscript Author Manuscript Author Manuscript

[12]. Zhu Y, Dai B, Li Y, Peng H, C5a and toll-like receptor 4 crosstalk in retinal pigment epithelial cells, Mol Vis 21 (2015) 1122–9. [PubMed: 26487798]

[13]. Appleton KM, Bigham KJ, Lindsey CC, Hazard S, Lirjoni J, Parnham S, Hennig M, Peterson YK, Development of inhibitors of heterotrimeric Galphai subunits, Bioorg Med Chem 22(13) (2014) 3423–34. [PubMed: 24818958]

[14]. Shyu HY, Ko CJ, Luo YC, Lin HY, Wu SR, Lan SW, Cheng TS, Hu SH, Lee MS, Ketamine Increases Permeability and Alters Epithelial Phenotype of Renal Distal Tubular Cells via a GSK-3β-Dependent Mechanism, J Cell Biochem 117(4) (2016) 881–93. [PubMed: 26365534]

[15]. Genewsky A, Jost I, Busch C, Huber C, Stindl J, Skerka C, Zipfel PF, Rohrer B, Strauss O, Activation of endogenously expressed ion channels by active complement in the retinal pigment epithelium, Pflugers Arch 467(10) (2015) 2179–91. [PubMed: 25427445]

[16]. Ishii M, Rohrer B, Bystander effects elicited by single-cell photo-oxidative blue-light stimulation in retinal pigment epithelium cell networks, Cell Death Discov 3 (2017) 16071. [PubMed: 28179989]

[17]. Valente AJ, Maddalena LA, Robb EL, Moradi F, Stuart JA, A simple ImageJ macro tool for analyzing mitochondrial network morphology in mammalian cell culture, Acta Histochem 119(3) (2017) 315–326. [PubMed: 28314612]

[18]. Watanabe H, Kuraya M, Kasukawa R, Yanagisawa H, Yanagisawa M, Fujita T, Analysis of C5a receptor by monoclonal antibody, J Immunol Methods 185(1) (1995) 19–29. [PubMed: 7665898]

[19]. Shutt T, Geoffrion M, Milne R, McBride HM, The intracellular redox state is a core determinant of mitochondrial fusion, EMBO Rep 13(10) (2012) 909–15. [PubMed: 22945481]

[20]. Song Z, Ghochani M, McCaffery JM, Frey TG, Chan DC, Mitofusins and OPA1 mediate sequential steps in mitochondrial membrane fusion, Mol Biol Cell 20(15) (2009) 3525–32. [PubMed: 19477917]

[21]. Yako T, Nakamura M, Nakamura S, Hara H, Shimazawa M, Pharmacological inhibition of mitochondrial fission attenuates oxidative stress-induced damage of retinal pigmented epithelial cells, J Pharmacol Sci 146(3) (2021) 149–159. [PubMed: 34030797]

[22]. Cai WJ, Chen Y, Shi LX, Cheng HR, Banda I, Ji YH, Wang YT, Li XM, Mao YX, Zhang DF, Dai PP, Sun XY, Ning XH, Huang SB, Ma JF, Zhao SF, AKT-GSK3beta Signaling Pathway Regulates Mitochondrial Dysfunction-Associated OPA1 Cleavage Contributing to Osteoblast Apoptosis: Preventative Effects of Hydroxytyrosol, Oxid Med Cell Longev 2019 (2019) 4101738. [PubMed: 31281574]

[23]. Frank M, Duvezin-Caubet S, Koob S, Occhipinti A, Jagasia R, Petcherski A, Ruonala MO, Priault M, Salin B, Reichert AS, Mitophagy is triggered by mild oxidative stress in a mitochondrial fission dependent manner, Biochim Biophys Acta 1823(12) (2012) 2297–310. [PubMed: 22917578]

[24]. Watanabe T, Saotome M, Nobuhara M, Sakamoto A, Urushida T, Katoh H, Satoh H, Funaki M, Hayashi H, Roles of mitochondrial fragmentation and reactive oxygen species in mitochondrial dysfunction and myocardial insulin resistance, Exp Cell Res 323(2) (2014) 314–25. [PubMed: 24631294]

[25]. Cheng G, Zielonka M, Dranka B, Kumar SN, Myers CR, Bennett B, Garces AM, Dias Duarte Machado LG, Thiebaut D, Ouari O, Hardy M, Zielonka J, Kalyanaraman B, Detection of mitochondria-generated reactive oxygen species in cells using multiple probes and methods: Potentials, pitfalls, and the future, J Biol Chem 293(26) (2018) 10363–10380. [PubMed: 29739855]

[26]. Jiang L, Tixeira R, Caruso S, Atkin-Smith GK, Baxter AA, Paone S, Hulett MD, Poon IK, Monitoring the progression of cell death and the disassembly of dying cells by flow cytometry, Nat Protoc 11(4) (2016) 655–63. [PubMed: 26938116]

[27]. Ishii M, Rohrer B, Bystander effects elicited by single-cell photo-oxidative blue-light stimulation in retinal pigment epithelium cell networks, 3 (2017) 16071.

[28]. Thurman JM, Renner B, Kunchithapautham K, Holers VM, Rohrer B, Aseptic injury to epithelial cells alters cell surface complement regulation in a tissue specific fashion, Adv Exp Med Biol 664 (2010) 151–8. [PubMed: 20238013]

Author Manuscript Author Manuscript Author Manuscript Author Manuscript

[29]. Schmidt RE, Gessner JE, Fc receptors and their interaction with complement in autoimmunity, Immunol Lett 100(1) (2005) 56–67. [PubMed: 16125792]

[30]. Davignon I, Catalina MD, Smith D, Montgomery J, Swantek J, Croy J, Siegelman M, Wilkie TM, Normal hematopoiesis and inflammatory responses despite discrete signaling defects in Galpha15 knockout mice, Mol Cell Biol 20(3) (2000) 797–804. [PubMed: 10629036]

[31]. Azevedo Voltarelli V, Coronado M, Goncalves Fernandes L, Cruz Campos J, Jannig PR, Batista Ferreira JC, Fajardo G, Chakur Brum P, Bernstein D, beta(2)-Adrenergic Signaling Modulates Mitochondrial Function and Morphology in Skeletal Muscle in Response to Aerobic Exercise, Cells 10(1) (2021).

[32]. Li Y, Li M, Yao G, Geng N, Xie Y, Feng Y, Zhang P, Kong X, Xue J, Cheng S, Zhou J, Xiao L, Telomerase inhibition strategies by siRNAs against either hTR or hTERT in oral squamous cell carcinoma, Cancer Gene Ther 18(5) (2011) 318–25. [PubMed: 21233858]

[33]. Parcellier A, Tintignac LA, Zhuravleva E, Hemmings BA, PKB and the mitochondria: AKTing on apoptosis, Cell Signal 20(1) (2008) 21–30. [PubMed: 17716864]

[34]. Chiara F, Rasola A, GSK-3 and mitochondria in cancer cells, Front Oncol 3 (2013) 16. [PubMed: 23386998]

[35]. Yang K, Chen Z, Gao J, Shi W, Li L, Jiang S, Hu H, Liu Z, Xu D, Wu L, The Key Roles of GSK-3beta in Regulating Mitochondrial Activity, Cell Physiol Biochem 44(4) (2017) 1445–1459. [PubMed: 29190615]

[36]. Zhang Q, Fu H, Zhang H, Xu F, Zou Z, Liu M, Wang Q, Miao M, Shi X, Hydrogen sulfide preconditioning protects rat liver against ischemia/reperfusion injury by activating Akt-GSK-3beta signaling and inhibiting mitochondrial permeability transition, PLoS One 8(9) (2013) e74422. [PubMed: 24058562]

[37]. Gomez L, Thiebaut PA, Paillard M, Ducreux S, Abrial M, Crola Da Silva C, Durand A, Alam MR, Van Coppenolle F, Sheu SS, Ovize M, The SR/ER-mitochondria calcium crosstalk is regulated by GSK3beta during reperfusion injury, Cell Death Differ 23(2) (2016) 313–22. [PubMed: 26206086]

[38]. Liu Y, Xu SQ, Long WJ, Zhang XY, Lu HL, C5aR antagonist inhibits occurrence and progression of complement C5a induced inflammatory response of microglial cells through activating p38MAPK and ERK1/2 signaling pathway, Eur Rev Med Pharmacol Sci 22(22) (2018) 7994–8003. [PubMed: 30536348]

[39]. de Brito OM, Scorrano L, Mitofusin 2 tethers endoplasmic reticulum to mitochondria, Nature 456(7222) (2008) 605–10. [PubMed: 19052620]

[40]. Liu Y, Zhu X, Endoplasmic reticulum-mitochondria tethering in neurodegenerative diseases, Transl Neurodegener 6 (2017) 21. [PubMed: 28852477]

[41]. Zauhar R, Biber J, Jabri Y, Kim M, Hu J, Kaplan L, Pfaller AM, Schäfer N, Enzmann V, Schlötzer-Schrehardt U, Straub T, Hauck SM, Gamlin PD, McFerrin MB, Messinger J, Strang CE, Curcio CA, Dana N, Pauly D, Grosche A, Li M, Stambolian D, As in Real Estate, Location Matters: Cellular Expression of Complement Varies Between Macular and Peripheral Regions of the Retina and Supporting Tissues, Front Immunol 13 (2022) 895519. [PubMed: 35784369]

[42]. Anderson DH, Radeke MJ, Gallo NB, Chapin EA, Johnson PT, Curletti CR, Hancox LS, Hu J, Ebright JN, Malek G, Hauser MA, Rickman CB, Bok D, Hageman GS, Johnson LV, The pivotal role of the complement system in aging and age-related macular degeneration: hypothesis revisited, Prog Retin Eye Res 29(2) (2010) 95–112. [PubMed: 19961953]

[43]. Rohrer B, Bandyopadhyay M, Beeson C, Reduced Metabolic Capacity in Aged Primary Retinal Pigment Epithelium (RPE) is Correlated with Increased Susceptibility to Oxidative Stress, Adv Exp Med Biol 854 (2016) 793–8. [PubMed: 26427491]

[44]. Feher J, Kovacs I, Artico M, Cavallotti C, Papale A, Balacco Gabrieli C, Mitochondrial alterations of retinal pigment epithelium in age-related macular degeneration, Neurobiol Aging 27(7) (2006) 983–93. [PubMed: 15979212]

[45]. Busch C, Annamalai B, Abdusalamova K, Reichhart N, Huber C, Lin Y, Jo EAH, Zipfel PF, Skerka C, Wildner G, Diedrichs-Mohring M, Rohrer B, Strauss O, Anaphylatoxins Activate Ca2+, Akt/PI3-Kinase, and FOXO1/FoxP3 in the Retinal Pigment Epithelium, Front Immunol 8 (2017) 703. [PubMed: 28663750]

Author Manuscript Author Manuscript Author Manuscript Author Manuscript

Highlights

- C5aR activation regulated mitochondrial dynamics and induced fusion events in resting cells.
- C5aR signaling increased mitochondrial fusion-related proteins MFN1 and MFN2, and OPA1 cleavage
- Mitochondrial fusion induced by C5aR activation was independent of mitochondrial ROS.
- C5aR-activation enhanced Gsk-3β-phosphorylation
- C5aR activation increased the number of mitochondria-ER contact sites.
- Treatment of cells with C5a prior to H_2O_2 exposure enhanced mitochondrial fragmentation and promoted nuclear pyknosis.
- Induction of oxidative stress in a single cell induced mitochondrial fragmentation in adjacent surrounding cells only in the presence of C5a.
- Mitochondrial fusion induced by C5aR activation sensitized the cell to a secondary damaging stimulus.

Author Manuscript Author Manuscript Author Manuscript Author Manuscript

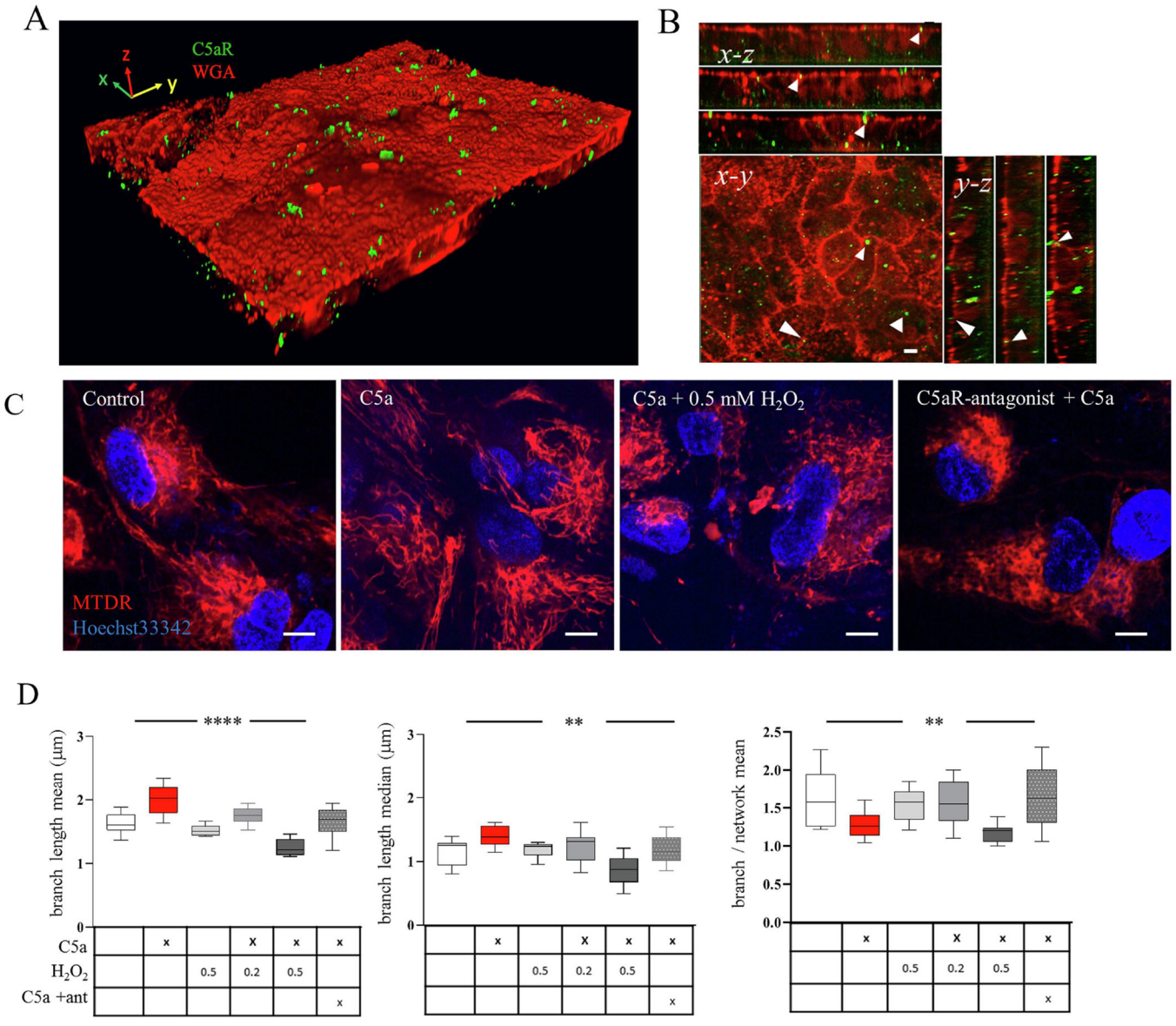

Figure 1. C5a receptor distribution and C5a-induced mitochondrial fusion.

(**A**) 3D-rendering of immunolabeling for C5aR (green) on cells labeled with Wheat Germ Agglutinin (WGA, red) for the identification of the apical cellular surface. (**B**) Orthogonal image reconstructed from x-y Z-stack images. C5aR fluorescence (green) colocalized with WGA fluorescence labeling the plasma membrane. Locations of the 3 sections are indicated in the x-y projection (arrows). (**C**) MitoTracker Deep Red (MTDR; red) was used to identify the mitochondrial network, Hoechst33342 (blue) labeled the nuclei for live-cell imaging. Stimulation of the C5aR with 52 nM of C5a induced mitochondrial fusion (second panel), addition of 0.5 mM H_2O_2 after C5a exposure enhanced fission (third panel), and pretreatment with C5aR-antagonist inhibited C5aR-induced fusion (fourth panel). Scale bar represents 10 µm. (**D**) Mitochondrial branch length mean (left graph) and median (middle graph) and the number of branches (right graph) per mitochondrion was analyzed using the MiNA (Mitochondrial Network Analysis) plugin, confirming the visual observations from

Author Manuscript Author Manuscript Author Manuscript Author Manuscript

1C. Boxplots depict the 25th to 75th percentiles and Whiskers show the 5–95th percentiles. Statistical analysis was performed using One-way ANOVA, ** 0.01, **** 0.0001.

Author Manuscript Author Manuscript Author Manuscript Author Manuscript

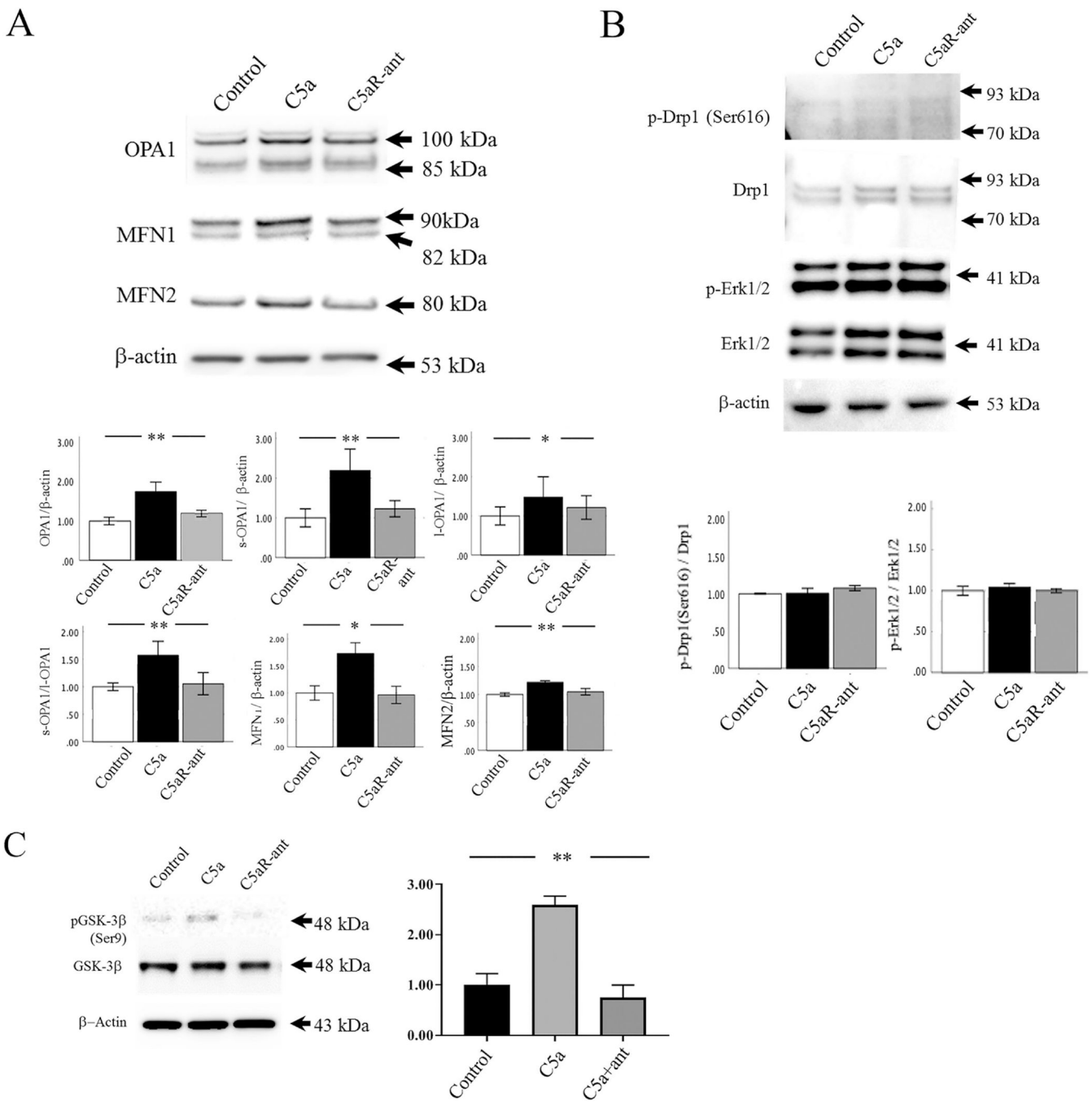

Figure 2. C5a-treatment altered levels of mitochondrial fission/fusion proteins analyzed using Western blotting.

(**A**) Western blots probed for mitochondrial fusion proteins, including the OPA1 cleavage products short chain (s-OPA1) and long chain OPA1 (l-OPA1), Mitofusin-1 (MFN1) and Mitofusin-2 (MFN2), and quantitative analysis of the blotting results documenting a significant increase in total OPA1 (=l-OPA1 + s-OPA1), l-OPA1 and s-OPA1 individually, as well as the s-OPA/l-OPA ratio together with an increase in MFN1 and MFN2 in response to C5a stimulation. Pre-treatment with the C5a antagonist normalized these proteins back to

Author Manuscript Author Manuscript Author Manuscript Author Manuscript

control levels. (**B**) Levels of the mitochondrial fission protein Drp1 and phosphorylated Drp1 at Ser616 (p-Drp1), together with its activator p-Erk1/2 (Thr202/Tyr204) were unaffected by C5a treatment, and quantitative analysis for the blotting results of 2C. (**C**) The activator of mitochondrial fusion, GSk-3β and phosphorylated Gsk-3β (p-Gsk-3β) at Ser9 was increased upon C5a treatment, and the quantification is provided. Across all experiments, the band intensity values were normalized with β-actin, and results compared with One-way ANOVA, * $p<0.05$, ** <0.01. Values in the charts represent mean ± S.E.M.

Author Manuscript Author Manuscript Author Manuscript Author Manuscript

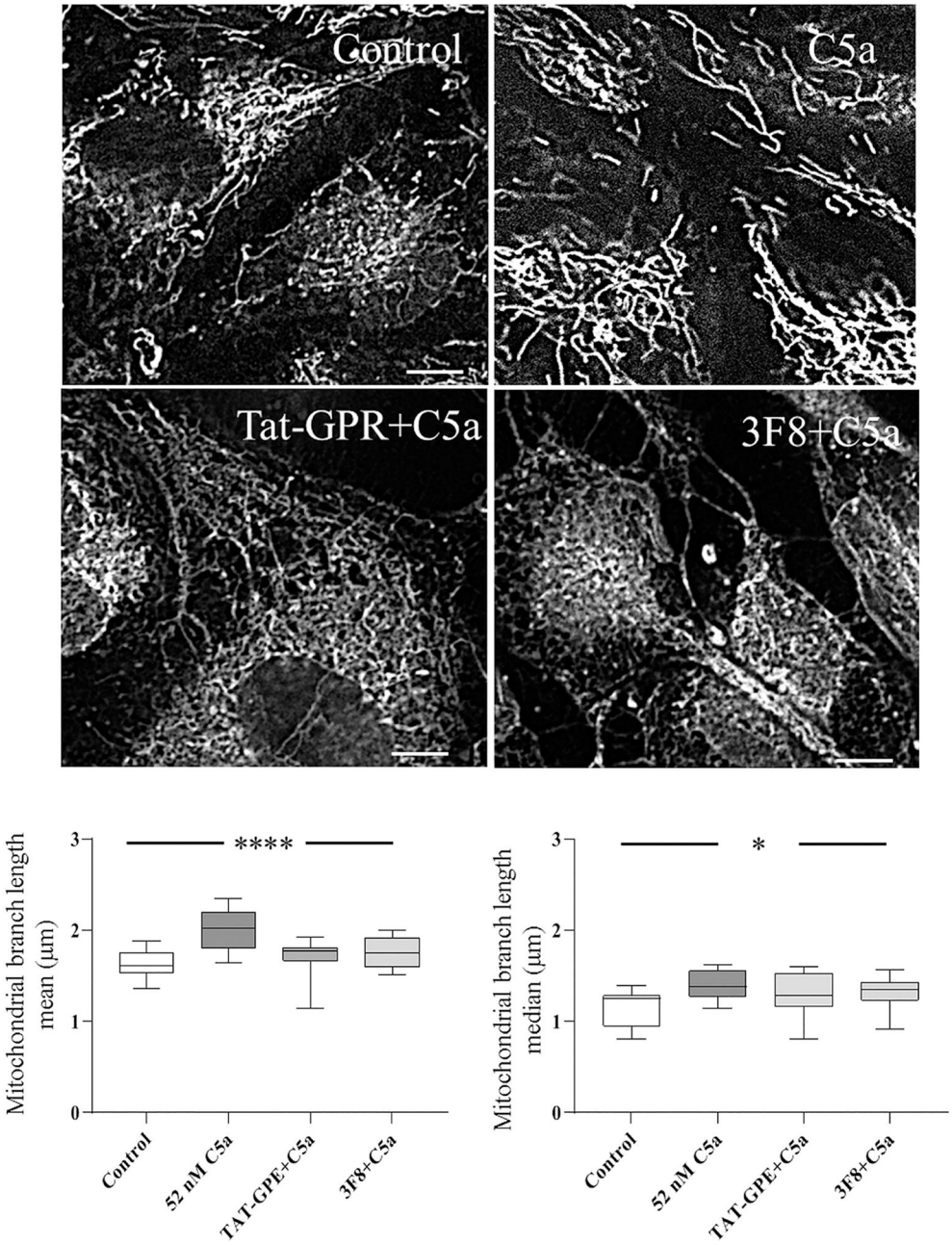

Figure 3. Examination of C5aR signaling in mitochondrial fusion, analyzing its G-protein, and downstream GSK-3β signaling.

(**A**) Confocal microscopy images comparing mitochondria-related fluorescence using MitoTracker Deep Red (MTDR) in control (upper left) and C5a-treated cells (upper right) document mitochondrial fusion in live-cell imaging. Pretreatment with the Gαi-specific inhibitor Tat-GPR (bottom left) and the Gsk-3β inhibitor 3F8 (bottom right) prevented C5a-induced mitochondrial fusion. (**B**) Quantification of mitochondrial mean (left graph) and median (middle graph) length as well as the mean number of branches per network (right graph) confirmed the visual observations. Box plot analysis was performed as described in

Author Manuscript Author Manuscript Author Manuscript Author Manuscript

Figure legend 1D. One-way ANOVA was applied for statistical analysis. p, *<0.05, **** < 0.0001. Scale bar in (**A**) represents 10 μm.

Author Manuscript Author Manuscript Author Manuscript Author Manuscript

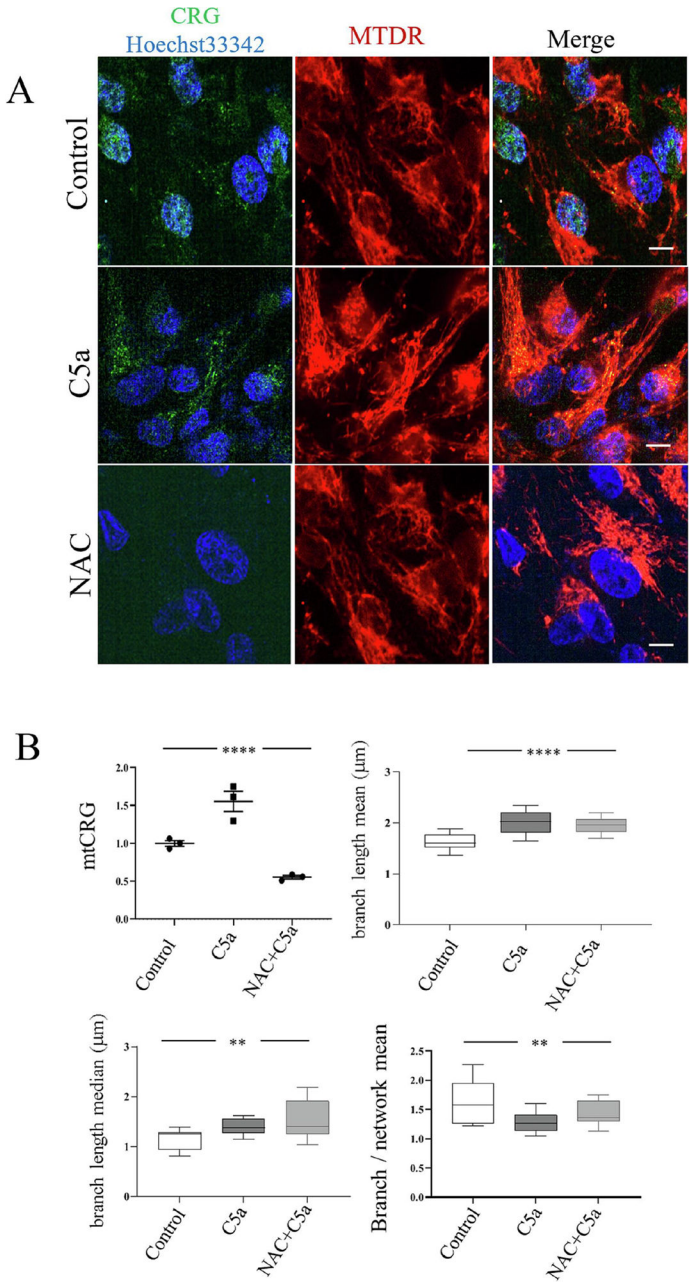

Figure 4. C5a-induced mitochondrial fusion is independent of mitochondrial reactive oxygen species (ROS) levels.

(**A**) Cells were labeled with CellRox Green (CRG, green) to detect ROS in mitochondria labeled with MitoTracker Deep Red (MTDR, red) for live-cell imaging. Mitochondrial ROS (mtROS) is defined by the colocalization of CRG and MTDR (yellow). C5a stimulation increased mtROS, which was prevented using the anti-oxidant NAC. (**B**) Quantitative analysis of mtROS, and mitochondrial branch length mean and median, and well as the number of branches per mitochondrion was assessed. While NAC prevented the C5a-induced rise in mtCRG, NAC had no effect on C5a-induced changes in mitochondrial network complexity. mtCRG level was normalized with mean of the control, and dots

represent individual values, and error bars depict their SEM. Mitochondrial mean and media length and number of branches per mitochondrion are shown as box and whiskers as described in Figure legend 1D. One-way ANOVA was applied for statistical analysis, ** p< 0.01, **** < 0.001. Scale bar in 3A represents 10 μm.

Author Manuscript Author Manuscript Author Manuscript Author Manuscript

Author Manuscript Author Manuscript Author Manuscript Author Manuscript

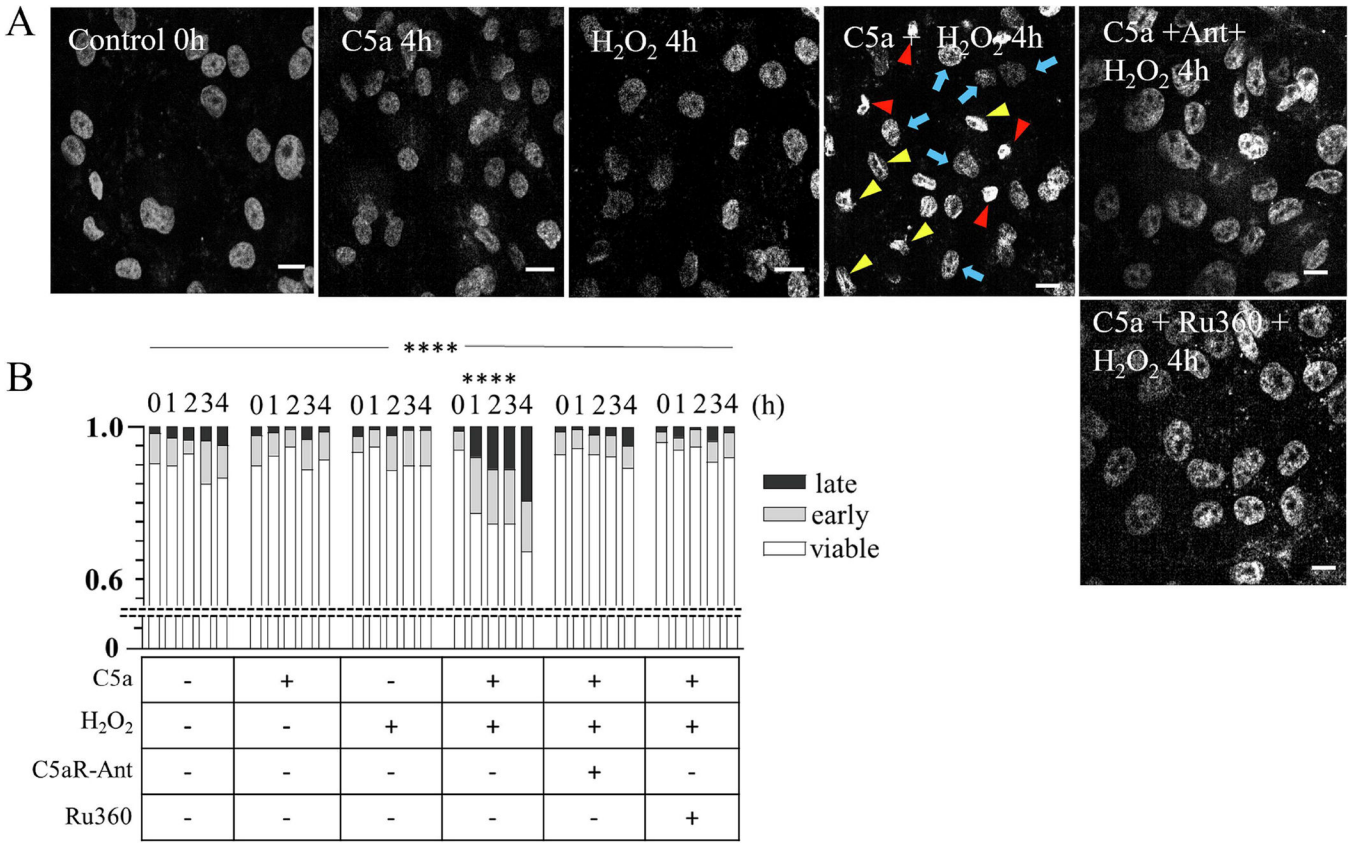

Figure 5. C5a-treatment sensitized the cells to exogeneous oxidative stress, leading to cell death.

(**A**) Nuclei were labeled with the nucleic acid stainToPro-3 for live cell imaging. Confocal images for are shown for control cells at 0 hour (first panel), and cells treated with 52 nM C5a (second panel), 0.5 mM H_2O_2 (third panel), C5aR-antagonist treatment prior to C5a exposure (fourth panel), and Ru360 treatment prior to C5a and H_2O_2 exposure, all at 4 hours. Nuclei were categorized based on fluorescence intensity into healthy (lowest intensity; blue arrows), early (intermediate; yellow arrow head), and late pyknosis (intense staining; red arrowhead) as documented in Figure S2. (**B**) Quantification for the number of early and late pyknotic nuclei as a fraction of all cells detected with ToPro-3 within an image over time (n=3 images each group). The values were analyzed with 2-way ANOVA in treatment and time factors **** $p<0.0001$. Scale bar in (**A**) represents 10 μm.

Author Manuscript Author Manuscript Author Manuscript Author Manuscript

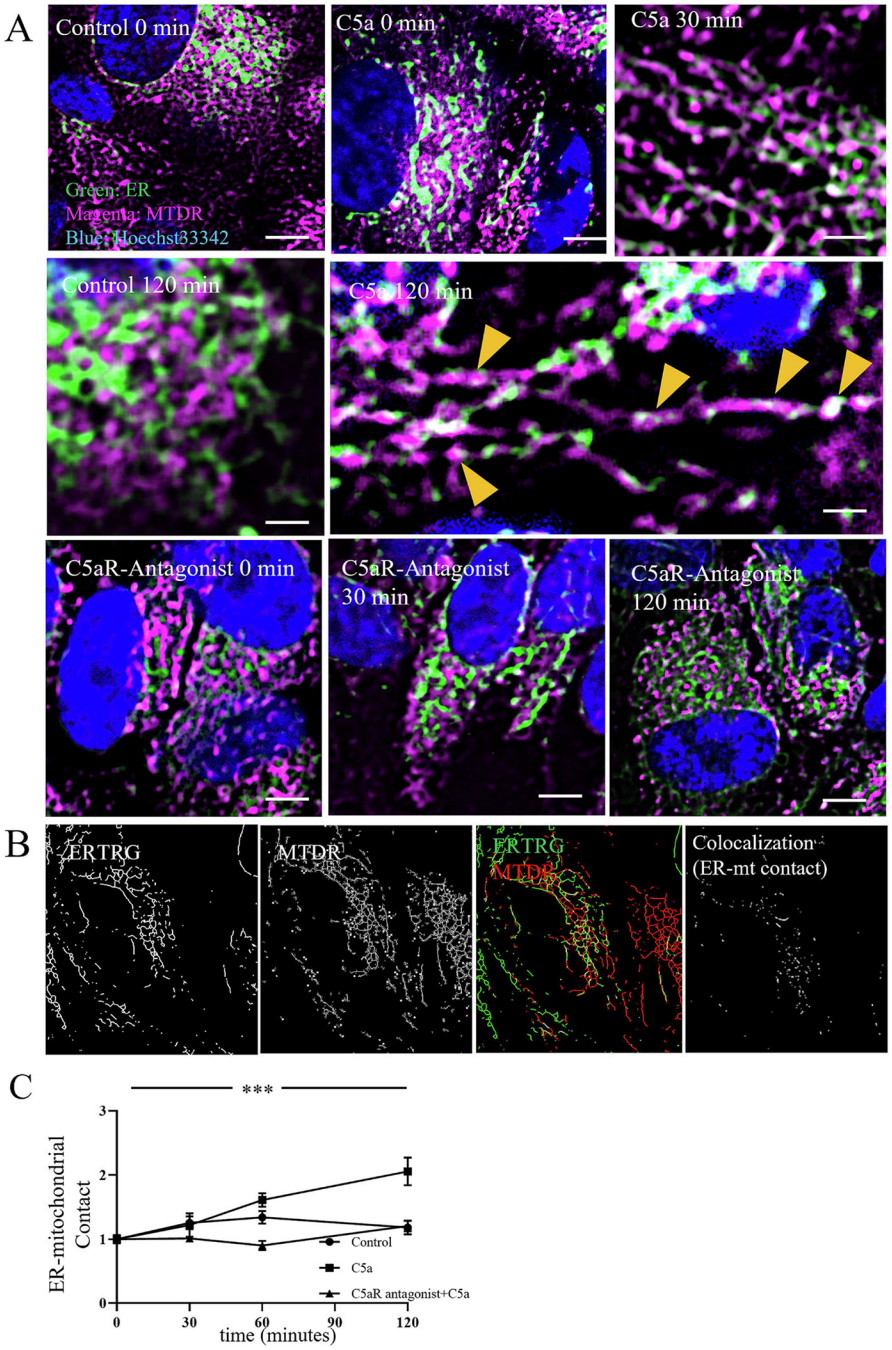

Figure 6. C5a-treatment increased the number of ER-mitochondrial contacts.

(**A**) Representative images of ER-mitochondria contacts in control cells and after C5a-treatment, collected at 0, 30, and 120 minutes in fixed monolayers. The endoplasmic reticulum (ER) was labeled with ERTracker Green (green), mitochondria were labeled with MitoTracker Deep Red (MTDR, false-colored in magenta), the nuclei were labeled with Hoechst33342 (blue). ER-mitochondria co-localizations between ERTR and MTDR was identified in white. The number of ER-mitochondria contact sites (yellow arrowheads) increased in the presence of C5a. The number of ER-mitochondria contact sites remained

Author Manuscript Author Manuscript Author Manuscript Author Manuscript

the same as in controls, if the cells are pretreated with C5aR antagonist prior to C5a exposure at 0, 30 and 120 minutes. (**B**) MTDR and ERTR images were converted to skeleton images and binarized using ImageJ plugins. Colocalization between MTDR and ERTR skeletons defined as ER-mitochondrial contacts loci were detected using the ImageJ colocalization plugin in ImageJ and quantified. (**C**) Changes of ER-mitochondrial contacts over time document the C5a effect. The raw values were normalized with the mean of the control at the zero time point. One-way ANOVA was used to analyze changes over time, *** $p < 0.001$. Scale bar in 6A represents 5 μm.

Author Manuscript
Author Manuscript
Author Manuscript
Author Manuscript

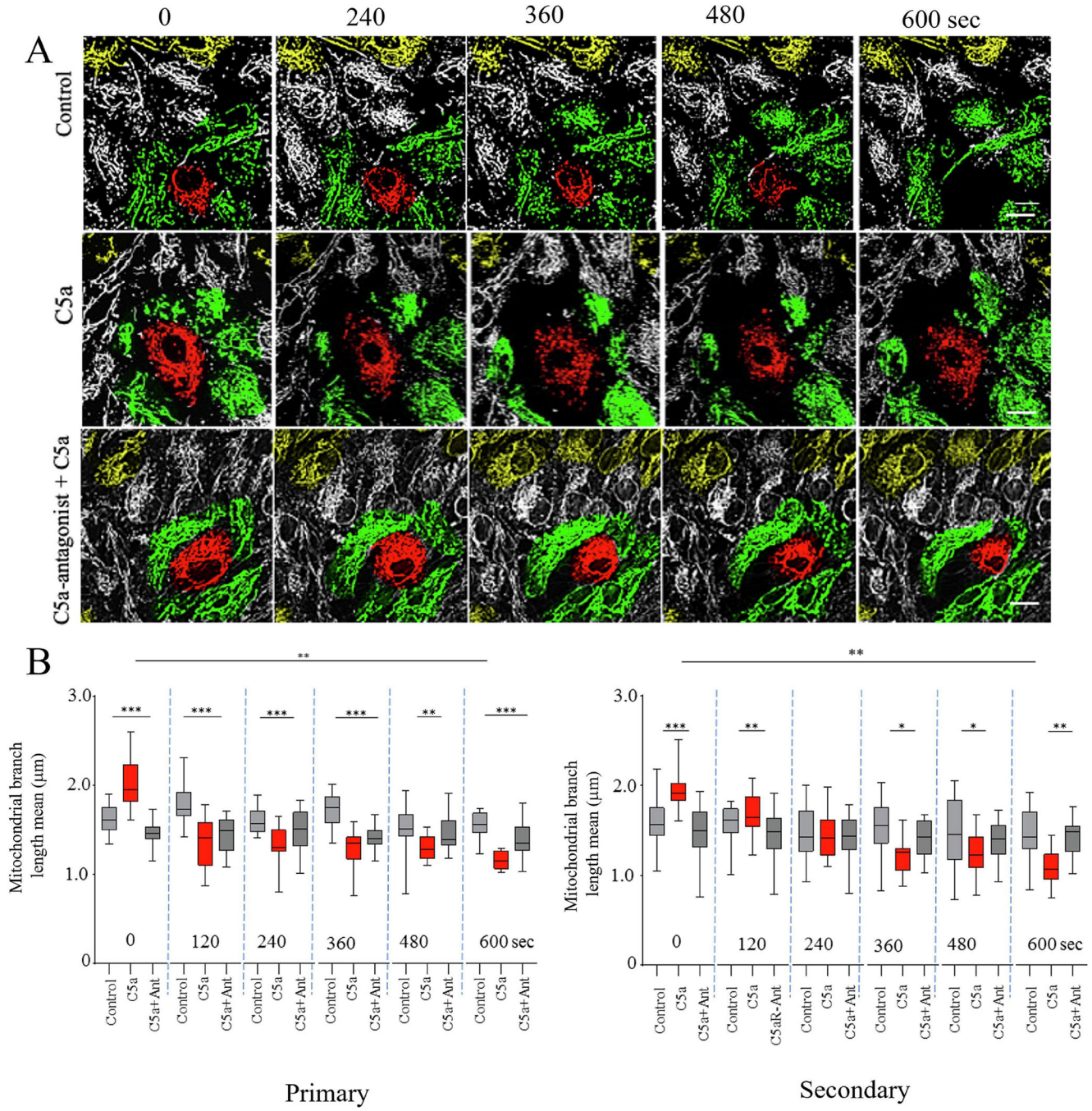

Figure 7. Blue spot laser stimulation on a single cell to trigger local oxidative stress induces mitochondrial fission in bystander cells in the presence of C5a.

(**A**) A 10% (38 kw/cm^2), 0.32 μm diameter 488 nm laser spot was used to stimulate a single cell (red) in an ARPE-19 monolayer network at 1 Hz for 10 minutes using live-cell imaging. The mitochondria in the surrounding cells in the monolayer were identified as primary surrounding cells (green), secondary surrounding cells (white) and others (yellow). Control cells, those exposed to C5a, and cells treated with C5aR antagonist + C5a were compared. C5a induced mitochondrial fission in primary and secondary surround cells, which could be

Author Manuscript Author Manuscript Author Manuscript Author Manuscript

inhibited by the C5aR antagonist. (**B**) Quantitative analysis of mean mitochondrial length in images captured every 120 seconds for primary surrounding (left graph) and secondary surrounding cells (right graph). Data are shown as box and whiskers as described in Figure legend 1D. While both primary and secondary surrounding cells treated with C5a at time point zero started with longer mitochondria, they rapidly fragmented when the center cell was stimulated with the blue laser. Mitochondria remained stable in control cells as well as those pretreated with C5aR antagonist. 2-way ANOVA was used to examine changes over time * $p<0.05$, **<0.01, ***<0.001. Scale bar in (**A**) represents 10 μm.

Author Manuscript Author Manuscript Author Manuscript Author Manuscript

Table 1.

Antibodies for immunolabeling and western blotting used in this study

TARGET	SOURCE	IDENTIFIER	Dilution
OPA1	Cell Signaling Technology	Cat# 80471, D6U6N	1:1000
Mitofusin-1	Cell Signaling Technology	Cat# 14739, D6E2S	1:1000
Mitofusin-2	Cell Signaling Technology	Cat# 11925, D1E9	1:1000
β-Actin	Cell Signaling Technology	Cat# 4970, 13E5	1:5000
p44/42 MAPK (Erk1/2)	Cell Signaling Technology	Cat# 4895, 137F5	1:1000
Phospho-p44/42 MAPK (Erk1/2) (Thr202/Tyr204)	Cell Signaling Technology	Cat# 4370, D13.14.4E	1:1000
GSK-3β	Cell Signaling Technology	Cat# 9315, 27C10	1:1000
Phosphor-Drp1 (Ser616)	Cell Signaling Technology	Cat# 4494, D3A4	1:1000
Drp1	Cell Signaling Technology	Cat# 8570, D6C7	1:1000
Phosphorylated-GSK-3β (Ser9)	Cell Signaling Technology	Cat# 9322, D3A4	1:1000
Goat Anti-rabbit IgG HRP-conjugate	Cell Signaling Technology	Cat# 7074	1:1000
C5a receptor	Biolegend	Cat # 344302 s1/2	1:1000 for WB 1:100 for ICC
Alexa fluor 488 anti-mouse Goat Antibody	Thermo Fisher	Cat # **A32723**	1:200